FARADAY

Formation and relaxation of $O_2(X^3\Sigma_g^-)$ in high vibrational levels ($18 \leqslant v \leqslant 23$) in the photolysis of O_3 at 266 nm

Kevin M. Hickson, Paul Sharkey, Ian W. M. Smith,* Andrew C. Symonds, Richard P. Tuckett and Gary N. Ward

School of Chemistry, The University of Birmingham, Edgbaston, Birmingham, UK B15 2TT

Using pulsed laser photolysis (PLP) and laser-induced fluorescence (LIF) we have studied the formation of $O_2(X^3\Sigma_g^-)$ in high vibrational levels when O_3 is photolysed at 266 nm. Experiments have been performed in both Ar and N_2 diluents. In the former, $O_2(X^3\Sigma_g^-)$ in high vibrational levels is formed primarily as a product of the reaction between $O(^1D)$ atoms and O_3: $O(^1D) + O_3 \rightarrow 2\ O_2(X^3\Sigma_g^-, v)$. In a large excess of N_2, the $O(^1D)$ atoms are quenched and one only observes the $O_2(X^3\Sigma_g^-)$ molecules created by direct photolysis in the 'triplet channel': $O_3 + h\nu$ ($\lambda = 266$ nm) $\rightarrow O_2(X^3\Sigma_g^-, v) + O(^3P)$. Employing LIF in the (0, v) and (2, v) bands of the O_2 ($B^3\Sigma_u^- - X^3\Sigma_g^-$) system, we have characterised the nascent vibrational distributions from both these processes for $18 \leqslant v \leqslant 23$. In addition, by observing how the population in specific vibrational levels changes with time, we have determined rate constants for vibrational relaxation of $O_2(X^3\Sigma_g^-, v = 21$ and 22) with He, O_2, N_2, CO_2, N_2O and CH_4. The results are compared with those obtained in other studies for relaxation from the same and other levels of $O_2(X^3\Sigma_g^-)$ and the implications of the results for atmospheric chemistry are discussed.

In 1988, Slanger *et al.*[1] reported the generation of large densities of ozone in laboratory experiments when pure O_2 was irradiated with unfocused laser radiation at 248 nm. They suggested that this process was probably initiated by weak two-photon dissociation of O_2 which led to O_3 being generated by combination of these atoms with molecules of O_2. Once O_3 was present, it would strongly absorb the laser radiation generating, amongst other products, O_2 in high vibrational levels of its $X^3\Sigma_g^-$ ground state. Slanger *et al.* proposed that the autocatalytic production of O_3 which they observed resulted from vibrationally excited O_2 molecules, in particular $O_2(X^3\Sigma_g^-, v = 7)$, absorbing 248 nm radiation and dissociating with the production of two $O(^3P)$ atoms *via* predissociation of the ($B^3\Sigma_u^-, v' = 2$) level. These atoms, as well as that formed by the initial dissociation of the O_3 molecule, would then combine with O_2 so that the photodissociation of one ozone molecule led to the production of three new ozone molecules. There is, of course, no reason why this process might not occur for a range of wavelengths between 200 and 300 nm under broadband UV illumination, so that the general mechanism can be written as:

$$O_3 + h\nu \rightarrow O_2(X^3\Sigma_g^-, v) + O(^3P) \quad (1a)$$

$$O_2(X^3\Sigma_g^-, v) + h\nu \rightarrow 2O(^3P) \quad (2)$$

$$3\{O(^3P) + O_2 + M \rightarrow O_3 + M\} \quad (3)$$

$$2h\nu + 3O_2 \rightarrow 2O_3$$

It should be noted that, although the 'triplet channel' represented by eqn. (1a) is not the major route for dissociation of O_3 between 200 and 300 nm, it does account for *ca.* 10% of the products,[2] the remainder resulting from the 'singlet channel':

$$O_3 + h\nu \rightarrow O_2(a^1\Delta_g) + O(^1D) \quad (1b)$$

The implications of their results for the photochemistry of the upper atmosphere did not escape Slanger *et al.*[1] They noted that there was, and still is, a discrepancy between the amounts of O_3 found in the mesosphere and upper stratosphere and the lower values predicted *via* photochemical models,[3–6] and they suggested that the mechanism represented by eqn. (1a)–(3) might bridge that gap.

The validity of such a proposal depends on three sets of quantities: (a) the quantum yields for production of $O_2(X^3\Sigma_g^-)$ in individual vibrational levels by process (1a); (b) the rates at which O_2 molecules in high vibrational levels are relaxed in collisions with other atmospheric gases, and (c) the rates of photodissociation from individual vibrational levels by solar radiation. Slanger *et al.*[1] estimated the rates of relaxation and photodissociation and concluded that their proposal of an 'additional' atmospheric mechanism for ozone generation was, at least, feasible. This conclusion was supported by Toumi *et al.*[7] Besides reporting some evidence for the presence of vibrationally excited O_2 in the upper atmosphere, they included the 'Slanger mechanism' in a numerical model and found that the rate of production of O_3 and its steady-state concentration in the upper atmosphere were significantly enhanced.

The calculations of both Slanger *et al.*[1] and Toumi *et al.*[7] made use of rate constants for the relaxation of $O_2(v)$ in collisions with $O_2(v = 0)$ that had been estimated[1] using the relatively simple theory of Rapp and co-workers.[8] It soon became clear that better estimates of these, and other, collisional relaxation rates for $O_2(v)$ were required if this mechanism for O_3 generation was to be properly assessed. Over the past several years, both experiments[6,9–12] and calculations[13,14] have addressed this problem. The present paper reports some of our own efforts in this direction.

The most direct and elegant method of preparing molecules in high levels of vibrational excitation for studies of collisional relaxation is that of stimulated emission pumping (SEP). Using a combination of 'pump' and 'dump' laser pulses, appreciable concentrations can be transferred to high vibrational levels in the electronic ground state of a molecule, if a suitable bound excited state exists. This method has been applied by Wodtke and co-workers[6,10,11] to obtain rate constants for vibrational relaxation of $O_2(v = 15$–$28)$ with a variety of collision partners.

In addition to optical pumping methods, exothermic photochemical and chemical reactions can be used to generate species in excited vibrational states.[9,11,15] The disadvantage is that molecules are produced over a range of states, often up to

the highest which is accessible energetically, and this distribution relaxes in a step-wise fashion down the manifold of vibrational levels. This cascade of population means that the kinetic behaviour of the populations in individual states becomes increasingly complicated the further a level is below the maximum populated in the pumping process. On the other hand, photochemical and chemical pumping methods are relatively easy to apply and have provided valuable information on relaxation from high vibrational levels in a variety of simple molecules.

In the present paper, we report state-specific rate constants for the relaxation of O_2 from levels $v = 21$, 22 in collisions with He, O_2, N_2, CO_2, N_2O and CH_4. To generate O_2 molecules in these v states, O_3 has been photolysed at 266 nm with the frequency-quadrupled output from an Nd:YAG laser. The energetics are such that the highest level which can be populated by process (1a) is $v = 22$. The kinetic behaviour of $O_2(v)$ was observed by following how the intensity of LIF signals excited in the (0, v) or (2, v) bands of the Schumann–Runge $B\,^3\Sigma_u^-$–$X\,^3\Sigma_g^-$ system changed as the time delay between the pulses of the photolysis and probe lasers was varied.

In addition to rate constants for the relaxation of $O_2(X\,^3\Sigma_g^-, v = 21, 22)$, we have measured the distributions of $O_2(X\,^3\Sigma_g^-)$ molecules over vibrational levels $18 \leqslant v \leqslant 23$ resulting from two processes: (1a), in which, as already stated, the energetics place a limit of $v = 22$ to the vibrational levels in O_2 which can be populated, and reaction (4) between $O(^1D)$, produced *via* the photodissociation channel (1b), and O_3.

$$O(^1D) + O_3 \rightarrow 2O_2(X\,^3\Sigma_g^-); \quad \Delta_r H^\circ = -581.6 \text{ kJ mol}^{-1} \quad (4a)$$

In these experiments, the delay between the pulses from the photolysis and probe lasers was set at a fixed small value and the frequency of the probe dye laser was scanned to record the intensities of several lines in two neighbouring vibrational bands in the $B\,^3\Sigma_u^-$–$X\,^3\Sigma_g^-$ system. In order to discriminate between the $O_2(X\,^3\Sigma_g^-, v)$ molecules produced by direct photolysis in process (1a) and those formed as the products of reaction (4a), experiments were performed in the presence of different bath gases. In argon, the $O(^1D)$ atoms generated in the singlet photolysis channel (1b) are only quenched relatively slowly and a large fraction react with O_3 so that the production of $O_2(X\,^3\Sigma_g^-, v)$ molecules is dominated by reaction (4a). In a large excess of nitrogen, however, $O(^1D)$ atoms are quenched in a process

$$O(^1D) + N_2 \rightarrow O(^3P) + N_2 \quad (5)$$

for which the rate constant at 298 K is $k_5 = 2.6 \times 10^{-11}$ cm^3 molecule^{-1} s^{-1}.[2] Since k_5 is 0.11 times the rate constant for total removal of $O(^1D)$ atoms by reaction with O_3,[2] in a 5000-fold excess of N_2 over O_3, 99.8% of the $O(^1D)$ atoms formed by photolysis of O_3 will be quenched and the $O_2(X\,^3\Sigma_g^-, v)$ molecules observed must be those formed in process (1a). Although it is known that both (1a) and (4a) create O_2 in high vibrational levels of the electronic ground state,[16–18] it is only recently that attempts to quantify these distributions have been made.[9,19–21] Our results are compared with those from these other recent studies.

Experimental

The experimental apparatus and method were similar to those employed by Smith *et al.*[15] and by Klatt and co-workers.[12] The reaction cell was constructed from Pyrex in the form of a cross. Gas mixtures of O_3 with the added relaxant and argon or nitrogen diluent were passed slowly through the main, 40 mm id, tube. A small fraction ($\leqslant$2%) of the O_3 was photolysed by the frequency-quadrupled output ($\lambda = 266$ nm) of an Nd : YAG laser (Spectron SL803 or SL403), typically generating *ca.* 10 mJ per pulse at 10 Hz. The beam from this laser and that from the probe dye laser entered the cell in counter-propagating directions through two side-arms, crossing the gas flow at right-angles. The side-arms carried baffles to reduce scattered laser light and any fluorescence from the windows at the end of the side-arms. Delays between the two laser pulses were controlled by a commercial delay generator (Stanford Research Systems, DG 535). The method of collecting and processing LIF signals has been described previously.[12,15]

Flows of the gases were controlled by mass flow controllers. The measurements were carried out at total pressures between 25 and 40 Torr using either argon or nitrogen as the buffer gas, present in large excess. In cases where it was necessary to add appreciable pressures of the relaxant, the flow of nitrogen was reduced accordingly to maintain a constant total pressure. All the experiments reported here were performed at room temperature, 295 $\pm$ 3 K.

To generate O_3, O_2 was passed, at a flow rate of *ca.* 200 l h^{-1}, through a commercial ozoniser (Fischer Ozon, model 500) operating at a current of 1 A. The products were then passed through a silica-gel (Fisons, 6–16 mesh) trap cooled with a CO_2–ethanol slush to *ca.* 200 K. This trap condensed the ozone, which was registered by the silica gel turning dark blue. Once sufficient O_3 had been gathered, the flow of O_2 was halted and the trap was pumped on with a rotary vacuum pump (Leybold, model D8A) protected by a foreline trap (Edwards, FL20K) containing activated charcoal (Aldrich, 4–12 mesh) to remove any ozone. The pump employed a synthetic oil (Watson and Bonnet, grade 500) to protect the pump against the effects of mixing hot organic oil with O_2.

All the other gases employed in these experiments were obtained from commercial suppliers and used without purification. Their sources and stated purities were as follows: argon (SIP, zero grade, 99.98 %); N_2 (BOC, 99.998%); helium (Air Products, 99.999%); O_2 (BOC, Industrial Grade, 99.9%); CO_2 (BOC, 99.8%); N_2O (SIP, 99.5%); CH_4 (SIP, 99–99.5%).

Analysis

(a) Relative vibrational populations

Fig. 1 shows a spectrum of the $B\,^3\Sigma_u^-$–$X\,^3\Sigma_g^-$ (0, 20) band of O_2 recorded 2 μs after the photolysis of 2 mTorr of O_3 diluted in 40 Torr of N_2. In general, to determine a ratio of populations in neighbouring vibrational levels, $N_v : N_{v-1}$, the intensities of four lines {typically, R(17), P(13), R(19) and P(15)} were recorded in two bands (0, v) and (0, $v - 1$) or (2, v) and (2, $v - 1$). Although both of the upper vibrational levels in these bands, *i.e.* $v' = 0$ and 2, are strongly predissociated, they have higher fluorescence quantum yields (Φ_F) than other vibrational levels in the $B\,^3\Sigma_u^-$ excited state. The values of Φ_F depend on the rotational, as well as the vibrational, level in $O_2(B\,^3\Sigma_u^-)$ varying from *ca.* (0.5–1) $\times 10^{-3}$ in $v' = 0$ and from *ca.* (1–2.5) $\times 10^{-4}$ in $v' = 2$.[9,22]

The area under each line was measured and was multiplied by a factor allowing for the difference in laser pulse energy at the two wavelengths. Each flux-normalised area was then divided by the appropriate Franck–Condon factor for the vibrational band used in the excitation process. Franck–Condon factors for the bands observed in the present work are listed in Table 1. Most of these were taken from the tabulation of Krupenie.[23] For those bands for which he did not report Frank–Condon factors, we calculated values using a program due to LeRoy[24] and the published RKR potential energy curves of Friedman[25] and Cheung *et al.*[26] Where a direct comparison between the two methods is possible, the agreement is excellent. Finally, corrected intensities for the

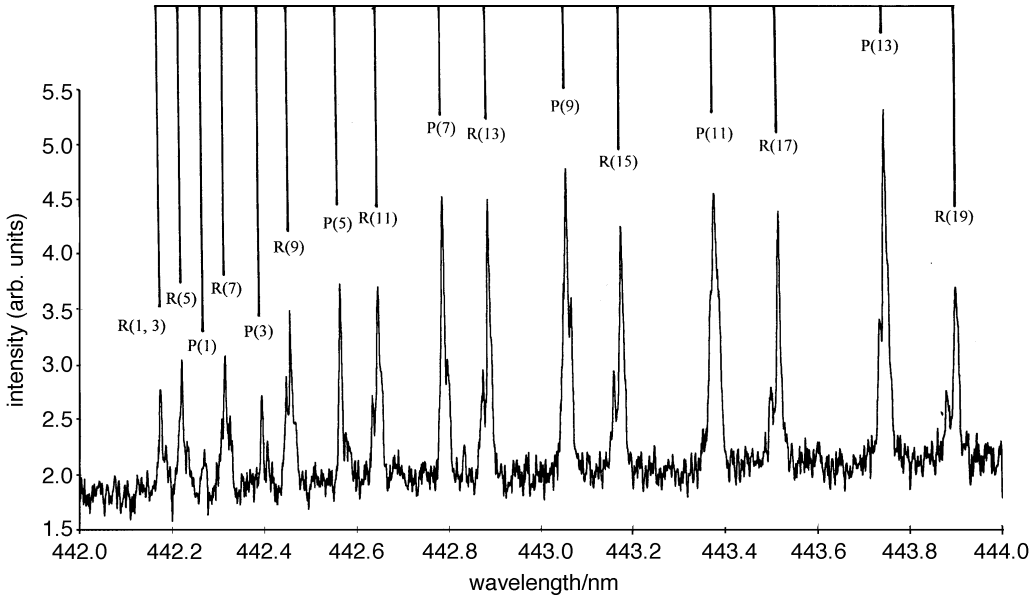

Fig. 1 Spectrum of the $B\,^3\Sigma_u^-$–$X\,^3\Sigma_g^-$ (0, 20) band of O_2 recorded 2 μs after the photolysis at 266 nm of 2 mTorr of O_3 in 40 Torr of N_2

same line in each of the two bands were ratioed and the average ratio of the four determinations was calculated. Since the upper rovibronic level was the same for each individual value of $N_v : N_{v-1}$ that was calculated, no correction was needed to allow for the different rates of predissociation from different rovibrational levels in the $B\,^3\Sigma_u^-$ state. For each value of v between 18 and 23 this experiment was repeated between three and five times and the final values of $N_v : N_{v-1}$ were calculated as a weighted average of these separate determinations.

(b) Relaxation rates

Each experiment provided a record of how the LIF signal from a selected rovibrational level of $O_2(X\,^3\Sigma_g^-)$ varied with time following photodissociation of O_3 with a pulse of laser radiation at 266 nm. As the total pressure was 25 or 40 Torr, rotational energy transfer was extremely rapid, so the signals directly reflected how $[O_2(v)]$, the concentration of O_2 in a specific vibrational level v of the $X\,^3\Sigma_g^-$ ground state, varied with time. Experiments were performed in a large excess of N_2 over O_3 and on $O_2(X\,^3\Sigma_g^-, v = 21$ and 22) which are the two highest levels accessible in the photodissociation process (1a).

As discussed in greater detail later, with most added collision partners, including N_2, relaxation occurs by processes involving changes of $\Delta v = 2$ in the excited O_2 molecule; *i.e.* $v = 22 \rightarrow 20$ and $21 \rightarrow 19$. Moreover, the rate constants for relaxation for $v = 22$ and $v = 21$ for most added relaxants have similar values. For these reasons, no allowance was made for the effects of cascading and the decays of LIF signal with time were fitted to single exponential functions to yield a pseudo-first-order rate constant for relaxation

$$k_{1st} = \sum_{M} k_M[M] \qquad (6)$$

where the summation is over all the species M (O_3, N_2 and any added gas) present in the gas mixture. In each series of experiments, [Q], the concentration of the added gas Q, was varied and a rate constant for relaxation by this species was obtained by plotting k_{1st} against [Q].

Results

(a) Relative vibrational populations

Table 2 summarises the results of our experiments designed to measure the distribution of $O_2(X, v)$ molecules over levels $18 \leqslant v \leqslant 23$. The errors quoted are statistical errors only; *i.e.* single standard deviations of the average value calculated from individual determinations based on pairs of the same rotational lines from neighbouring bands. In the presence of large excesses of N_2, $[N_2] : [O_3] \geqslant 5000$, there is no significant variation in the ratios of populations in neighbouring vibrational levels and no signals could be measured from $v = 23$. These observations are consistent with the $O(^1D)$ atoms produced by photolysis of O_3 at 266 nm *via* the singlet channel being completely quenched by N_2 so that the vibrationally excited O_2 is formed entirely by O_3 photolysis *via* the

Table 1 Franck–Condon factors for vibrational bands within the ($B\,^3\Sigma_u^-$–$X\,^3\Sigma_g^-$) Schumann–Runge system of O_2

v', v''	band origin/nm[a]	Franck–Condon factors[a]	Franck–Condon factors[b]
0, 17	384.1	7.42 (−2)[c]	7.31 (−2)
0, 18	402.1	4.37 (−2)	4.28 (−2)
0, 19	421.5	2.21 (−2)	2.22 (−2)
0, 20	442.3	9.59 (−3)	9.32 (−3)
0, 21	464.9	3.52 (−3)	3.42 (−3)
0, 22	489.1	—	1.06 (−3)
0, 23	515.4	—	2.72 (−4)
2, 21	437.3	1.26 (−1)	1.26 (−1)
2, 22	458.7	—	1.00 (−1)
2, 23	481.7	—	6.09 (−2)

[a] From ref. 23; [b] calculated *via* an RKR method using a program supplied by LeRoy[24] and the published potential-energy curves from ref. 25 and 26; [c] 7.42 (−3) ≡ 7.42×10^{-3}, *etc.*

Table 2 Relative vibrational populations of $O_2(X\,^3\Sigma_g^-)$ observed in argon diluent, and in large excess concentrations of N_2

N_v/N_{v-1}	Ar diluent	N_2 diluent	$[N_2]:[O_3]$	from ref. 9[c]
N_{23}/N_{22}[a]	1.17 ± 0.26	0	5 000	
N_{22}/N_{21}[a]	1.46 ± 0.27	0.50 ± 0.16	8 000	
		0.63 ± 0.25	5 000	0.68[a]
		0.54 ± 0.13[d]		
N_{21}/N_{20}[b]	1.20 ± 0.09	1.03 ± 0.22	20 000	
		0.84 ± 0.07	10 000	
		0.98 ± 0.16	5 000	
		0.92 ± 0.06[d]		0.81[b]
N_{20}/N_{19}[b]	2.50 ± 0.14	1.98 ± 0.18	20 000	
		2.01 ± 0.18	11 000	
		2.06 ± 0.12	5 000	
		2.02 ± 0.09[d]		1.15[b]
N_{19}/N_{18}[b]	1.42 ± 0.11	1.11 ± 0.15	20 000	
		1.27 ± 0.06	5 000	
		1.21 ± 0.06[d]		1.51[b]

[a] Determined by measuring line intensities in the (2, v) and (2, $v-1$) bands. [b] Determined by measuring line intensities in the (0, v) and (0, $v-1$) bands. [c] With $[N_2]:[O_3] = 3000$. [d] Weighted averages and weighted single standard deviations from the determinations with $[N_2]:[O_3] \geqslant 5000$.

triplet channel. In the absence of N_2, the signals from $O_2(X\,^3\Sigma_g^-, 18 \leqslant v \leqslant 23)$ are much stronger and clearly dominated by the production of vibrationally excited molecules in reaction (4a) of the $O(^1D)$ atoms with O_3.

The partial vibrational distributions that we have determined in our experiments are displayed in Fig. 2. We shall compare these results with similar data from other studies in the next section.

(b) Rates of relaxation of $O_2(X\,^3\Sigma_g^-, v = 21, 22)$

Fig. 3 shows examples of traces of the LIF signals from $O_2(v = 21)$ formed by photolysis of O_3 in a large excess of N_2. He is present as an added relaxant. Fig. 4 displays a plot of k_{1st}, the pseudo-first-order rate constants for relaxation, for $O_2(v = 21)$ *versus* [He]. It can be seen that, even in the absence of added relaxant, the value of k_{1st} is large. Under these conditions, there will be two terms contributing to the measured value of k_{1st}, *cf.* eqn. (6), corresponding to relaxation by O_3 and by N_2. Relaxation by O_3 is rapid, Mack *et al.*[11] report a rate constant for relaxation of $O_2(v = 21)$ by O_3 of 5.5×10^{-12} cm^3 molecule^{-1} s^{-1}. Almost certainly, the fast rate of relaxation reflects the possibility of single quantum near-resonant V–V transfer to the ν_1 (1110 cm^{-1}) and ν_3 (1042 cm^{-1}) modes of O_3. Although relaxation by N_2 is intrinsically slow (see below), its concentration is high in our experiments.

In each series of experiments the concentrations of O_3 and N_2 are kept constant. Therefore, the gradients of such plots yield second-order rate constants for relaxation by the added

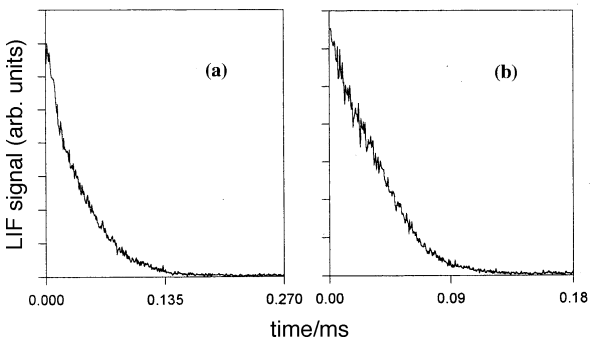

Fig. 3 Examples of LIF signals from $O_2(v = 21)$ in the presence of different concentrations of added helium: (a) [He] = 2.3×10^{16} molecule cm^{-3}; (b) [He] = 1.28×10^{17} molecule cm^{-3}

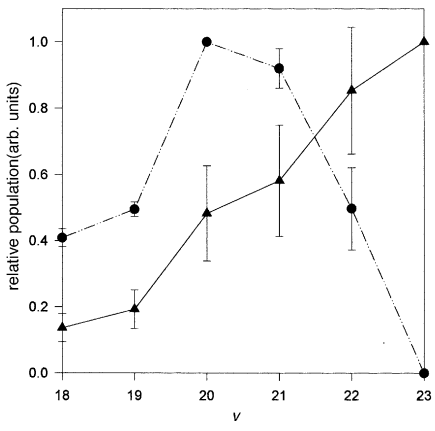

Fig. 2 Relative populations of $O_2(X\,^3\Sigma_g^-, 18 \leqslant v \leqslant 23)$ observed following the photolysis of O_2 at 266 nm in a large excess of N_2 (●) and in a large excess of Ar (▲)

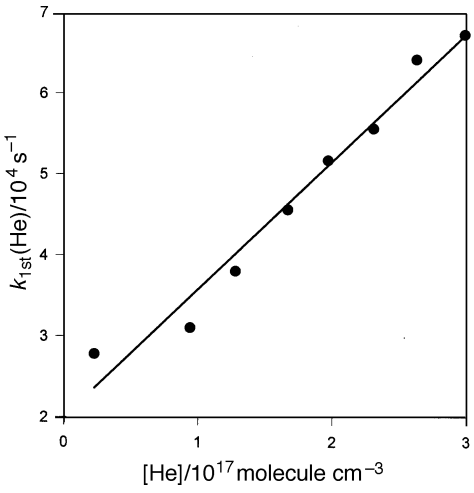

Fig. 4 Variation of the first-order rate constants for relaxation of O_2 ($v = 21$) in the presence of different concentrations of helium

Table 3 Rate constants (k/cm^3 molecule^{-1} s^{-1}) and collisional transfer probabilities (P_M^v)[a] for the relaxation of $O_2(v = 21$ and 22) by He, O_2, N_2, CO_2, N_2O and CH_4

collision partner	$v = 21$	$v = 22$
He	$1.6_5 \pm 0.1\ (-13)^{b,c}$ 4.2 (−4)	$2.6 \pm 0.1\ (-13)$ 6.7 (−4)
O_2	$3.8 \pm 0.45\ (-15)$ 1.6 (−5)	$4.4 \pm 1.0\ (-15)$ 1.8 (−5)
N_2	$1.0 \pm 0.3\ (-14)$ 3.7 (−4)	$4.3 \pm 0.8\ (-15)$ 1.5 (−4)
CO_2	$1.4 \pm 0.7\ (-13)$ 5.4 (−4)	$5 \pm 2\ (-14)$ 1.9 (−4)
N_2O	$2.7 \pm 0.9\ (-12)$ 1.0 (−2)	$1.1 \pm 0.2\ (-12)$ 4.1 (−3)
CH_4	$1.4 \pm 0.5\ (-12)$ 4.2 (−3)	$7.6 \pm 0.5\ (-13)$ 2.3 (−3)

[a] P_M^v is set equal to k/Z°, where Z°, the rate constant for collisions between hard-spheres, is calculated using hard-sphere collision diameters taken from J. O. Hirschfelder, C. F. Curtiss and R. B. Bird, *Molecular Theory of Gases and Liquids*, Wiley, New York, 1954. [b] $1.4 \pm 0.2\ (-14) \equiv (1.4 \pm 0.2) \times 10^{-14}$, *etc.* [c] The rate constants quoted are weighted averages of the values determined from between two and six series of experiments in each of which several first-order rate constants were measured at different concentrations of a given relaxant. The errors are cited at the level of single standard deviations. They correspond to whichever is the larger of the weighted error or the mean error of individual determinations from the weighted mean.

gas, *i.e.* in the example given, for

$$O_2(v = 21) + He \rightarrow O_2(v < 21) + He \qquad (7)$$

Table 3 summarises the results that we have obtained for the relaxation of $O_2(v = 21)$ and $O_2(v = 22)$ from experiments of this kind.

Discussion

The vibrational distribution of $O_2(X\,^3\Sigma_g^-, v)$ produced in the photolysis of ozone is fundamentally interesting and may be of considerable importance in atmospheric chemistry. The experimental approaches that have been adopted to investigate this problem have been of two kinds. Our own experiments are similar to those of Slanger and co-workers.[9] They photolysed O_3 at 248 nm using the output from a KrF excimer laser and observed relative vibrational level populations in $O_2(X\,^3\Sigma_g^-)$ using LIF. As Fig. 5 shows, they inferred rather different distributions depending on whether they measured the relative LIF intensities in the (0, v) or (2, v) vibrational bands. Our own measurements for $v = 18$–22 from the direct photodissociation process (1a) fall somewhere between the two distributions reported by Slanger and co-workers.[9]

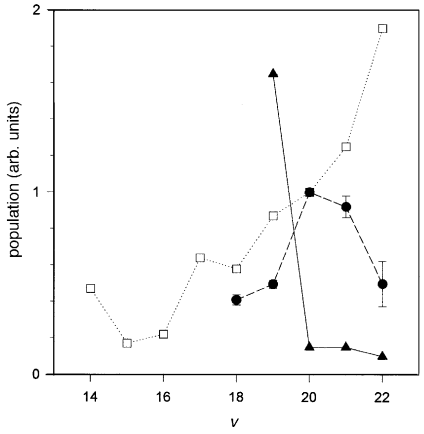

Fig. 5 Comparison of the vibrational distribution of O_2 ($X\,^3\Sigma_g^-$, $18 \leqslant v \leqslant 22$) from O_3 photolysis at 266 nm determined in the present experiments (●) with those reported by Park and Slanger[9a] using the (0, v) bands (▲) and the (2, v) bands (□)

They noted that reaction (4) between $O(^1D)$ and O_3 could also produce highly excited $O_2(X\,^3\Sigma_g^-, v)$ and, therefore, like ourselves, carried out their experiments in a large excess ($\geqslant 3000$) of N_2 or O_2 over O_3 in order to quench the $O(^1D)$ atoms. Consequently, the reasons for the differences between our distribution and theirs, or indeed for the differences between the two distributions which they report, are not entirely clear. However, we do note that the agreement between our values of $N_v : N_{v-1}$ (column 3 of Table 2) and those which Slanger and co-workers obtained using the same pair of bands as we used (column 5 of Table 2) is rather better than might be suggested from the comparison shown in Fig. 5.

The technique of photofragment spectroscopy has also been applied to a study of the partitioning of energy among the products of ozone photodissociation.[19–21] The most recent and extensive experiments of this kind have been those of Miller *et al.*[21] using an ion imaging technique. In the measurements reported so far,[21] O_3 in a molecular beam was photolysed by pulsed laser radiation at 226 nm. This serves both to dissociate the O_3 and to ionize the $O(^3P_2)$ fragment through a 2 + 1 REMPI (resonance enhanced multiphoton ionisation) process. From the two-dimensional images of the O^+ ions accelerated onto a phosphor screen the distribution of relative translational energies of the products could be deduced, and the internal state distribution of the $O_2(X\,^3\Sigma_g^-)$ fragment inferred through energy balance. For photolysis at 226 nm, these two distributions were bimodal. The vibrational state distributions of O_2 for $19 \leqslant v \leqslant 26$ close to the highest accessible level ($v = 27$) were confirmed by pulse–probe LIF measurements[21] of the kind that we report here. Although the two distributions needed normalising with respect to one another, the agreement between the two sets of results is impressive.

Houston's group have now carried out similar experiments using ion imaging over a range of photolysis wavelengths using separate lasers to effect the photodissociation of O_3 and to ionise the product $O(^3P_2)$ atoms.[27] In Fig. 6, we show the vibrational distribution of $O_2(X\,^3\Sigma_g)$ deduced from their measurements of the translational energies of $O(^3P_2)$ formed in photolysis of O_3 at 266 nm; *i.e.* at the same wavelength as used in the present experiments. Superimposed on this distribution are our own measurements of the vibrational populations in $18 \leqslant v \leqslant 22$. The agreement is only moderately satisfactory. Some of the difference, particularly at the highest levels, may arise from the fact that we are not comparing like with like, as the rotational and possibly vibrational temperatures in the two experiments are quite different.

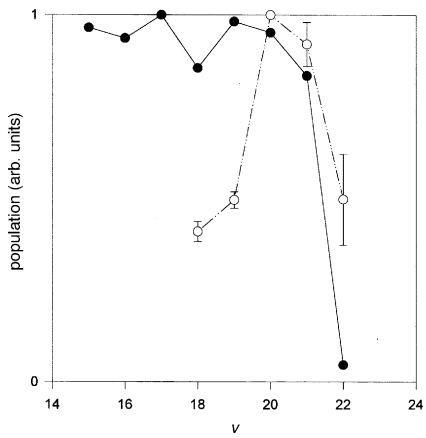

Fig. 6 Comparison of the vibrational distribution of $O_2(X\,^3\Sigma_g^-$, $18 \leqslant v \leqslant 22$) from O_3 photolysis at 266 nm determined in the present experiments (○) with the distribution deduced from the ion imaging experiments of Houston and co-workers[27] (●) in which O_3 was photolysed in a molecular beam and the translational energy distribution of $O(^3P_2)$ atoms was measured

Although it has been known for many years[16–18] that reaction (4a) creates O_2 in highly vibrationally excited levels of the $X\,^3\Sigma_g^-$ state, there has apparently been no attempt to measure the vibrational distribution in what might be termed the laser era. Cleveland and Wiesenfeld[18a] reported the observation of $O_2(X\,^3\Sigma_g^-,\ v = 14–16$ and $18–22)$ using LIF in the Schumann–Runge system. However, they did not clearly distinguish formation in reaction (4a) from production *via* the triplet photodissociation channel (1a), nor did they make any effort to measure the relative populations in different vibrational levels.

Reaction (4a) is very strongly exothermic. Indeed, reaction between $O(^1D)$ and O_3 can generate two $O(^3P)$ atoms:

$$O(^1D) + O_3 \rightarrow O_2(X\,^3\Sigma_g^-) + 2O(^3P); \qquad \Delta_r H^\circ = -83.1 \text{ kJ mol}^{-1} \quad (4b)$$

and it has been reported[28] that this reaction and reaction (4a) have equal rates. We have observed $O_2(X\,^3\Sigma_g^-)$ populations over a rather narrow range of high vibrational levels which, on energetic grounds, cannot be produced in reaction (4b) and must result from reaction (4a). The energies of the levels at the limits of this range, *i.e.* $v = 18$ and $v = 23$, correspond to 50.4% and 61.6%, respectively, of the energy released in reaction (4a). The observation that the vibrational populations increase monotonically from $v = 18$ to $v = 23$ suggests that a high proportion of the energy released in reaction (4a) is deposited into the vibration of one of the $O_2(X\,^3\Sigma_g^-)$ product molecules. Therefore it seems likely that the reaction proceeds by a direct mechanism with the other O_2 product being vibrationally unexcited.

In our studies of vibrational relaxation of $O_2(X\,^3\Sigma_g^-)$, the only atomic collision partner for which relaxation rates have been measured is helium. In this case, only V–T,R (vibration–translation, rotation) energy transfer is possible and it is expected to occur by a single quantum transition; *i.e.*

$$O_2(v = 22) + He \rightarrow O_2(v = 21) + He \quad (7a)$$

and

$$O_2(v = 21) + He \rightarrow O_2(v = 20) + He \quad (7b)$$

for which the transition energies correspond to 1067 cm^{-1} for $v = 22$ to 21 and 1091 cm^{-1} for $v = 21$ to 20.[23] For such V–T,R processes, it is expected that the collisional probability for energy transfer involving the same vibrationally excited molecule will increase as the reduced mass of the collision pair falls and this has been observed for O_2 $(v = 1)$,[29] as well as for other molecules in low-lying vibrationally excited states.[30] In all cases, He is found to be appreciably more effective as a relaxant than the other noble gases.

The increase in rate constant with v, which is found for the relaxation of $O_2(X\,^3\Sigma_g^-, v)$ by He as v increases from 1 to 22, has two principal sources. First, the vibrational matrix elements for $v \rightarrow v - 1$ increase approximately linearly with v. Making allowance for this factor yields values of $(P_{v,\,v-1}/v)$, the 'reduced probabilities' for V–T,R energy transfer. We have reported before,[12] and show in Fig. 7, that $(P_{v,\,v-1}/v)$ increases by a factor of *ca.* 1.8 from $O_2(v = 1)$ to $O_2(v = 10)$. There is a further increase as v is raised to the levels $v = 21$ and 22 that have been studied in the present work, and within experimental error, $(P_{v,\,v-1}/v)$ rises monotonically from $v = 1$ to 22. The second effect, which causes the increase in reduced probabilities, is that vibrational anharmonicity decreases the spacing between neighbouring vibrational levels. Thus, $\Delta E/hc$ for $v = 1$ to 0 is 1556.4 cm^{-1}, whereas it is only 1067 cm^{-1} for $v = 22$ to 21.

With molecular collision partners, $O_2(v)$ can relax by intermolecular V–V energy exchange if the vibrational transition energies are not too different. Self-relaxation, *i.e.* relaxation of $O_2(v)$ by $O_2(v = 0)$, is an especially interesting case. As v increases the vibrational transition energy $\Delta E_{v,\,v-1}$ decreases. Consequently, the V–V process

$$O_2(v) + O_2(v = 0) \rightarrow O_2(v - 1) + O_2(v = 1) \quad (8)$$

becomes increasingly less resonant and more endothermic. As a result, the rate constants for relaxation fall between $v = 8$ and $v = 20$, as shown in Fig. 8. The calculations of Hernandez *et al.*[14] show this effect clearly. At $v = 19$, however, the rate constants for V–T,R relaxation, which increase with v as the spacings between neighbouring levels become smaller, become larger than those for V–V relaxation. Therefore V–T,R energy transfer is dominant at higher vibrational levels. In this respect, it is interesting to note that the rate constants for relaxation of $O_2(v = 21$ and $22)$ by $O_2(v = 0)$ are *ca.* 50 times smaller than those for relaxation of the same levels by helium. This is a clear demonstration of how V–T,R relaxation is exceptionally facile when the reduced mass of the collision pair is unusually small.

In Fig. 8, we compare the experimental data from our laboratory, both the results reported in the present paper and the rate constants for $O_2(8 \leqslant v \leqslant 11) + O_2(v = 0)$,[12] with the rate constants reported by Slanger and co-workers[9] and those determined by Wodtke and co-workers.[6,10,11] Our present

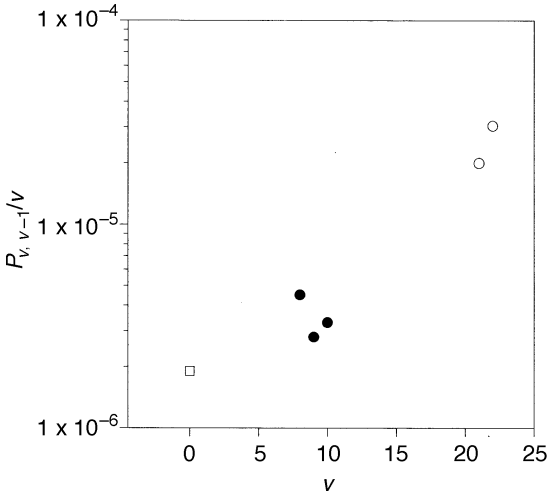

Fig. 7 Reduced probabilities, $(P_{v,\,v\text{-}1}/v)$, for relaxation of $O_2(X\,^3\Sigma_g^-, v)$ by helium plotted *vs.* v: results from the present work (○), from the measurements of Klatt and co-workers[12] (●) and from Millikan and White (□)[29]

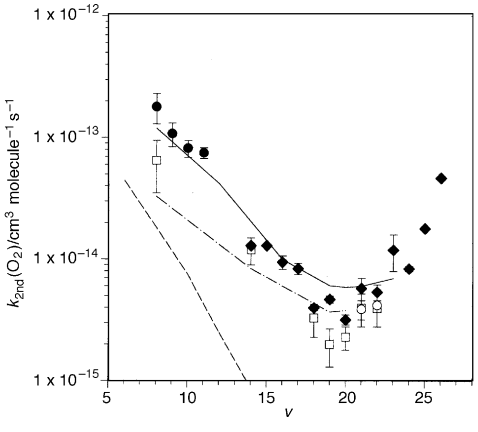

Fig. 8 Rate constants for the relaxation of $O_2(v)$ by O_2 plotted *vs.* v. The symbols show the results of the present work including estimated uncertainties (○), and the measurements of Slanger and co-workers[9] (□), Klatt and co-workers[12] (●) and Mack *et al.*[11] (◆). The lines show the results of various theoretical calculations: (– – –) Slanger *et al.*,[1] as cited by Toumi *et al.*;[7] (— · — · —) Billing and Kolesnick;[13] (———) Hernandez *et al.*[14]

experiments are similar in kind to those of Slanger and co-workers and the two sets of results are in excellent agreement. Both sets of rate constants are slightly lower than those from Wodtke's laboratory. As stated earlier, Wodtke's data are the most extensive set yet obtained for the relaxation of O_2 in high vibrational states. Furthermore, the method employed is very direct since the use of stimulated emission pumping populates single high vibrational levels in the $X\,^3\Sigma_g^-$ electronic ground state of O_2. It has been suggested[9] (but see below) that the sharp increase in rate constants at and above $v = 26$ may be due to the onset of chemical reaction , *i.e.*

$$O_2(X\,^3\Sigma_g^-, v \geqslant 26) + O_2 \rightarrow O_3 + O(^3P) \qquad (9)$$

Fig. 9–11 compare three sets of results for the relaxation of vibrationally excited O_2 by N_2, CO_2 and N_2O from our earlier data[12] for vibrational relaxation of $O_2(8 \leqslant v \leqslant 11)$, the present results for $O_2(v = 21$ and $22)$ and the extensive data of Mack *et al.*[11] As with O_2, our data are in reasonable agreement with the results obtained using the stimulated emission pumping technique. For all three of these collision partners, it appears that the dominant relaxation mechanism at and around O_2 vibrational levels $v \approx 20$ may be a near-resonant V–V energy exchange process, such as

$$O_2(v) + N_2(v = 0) \rightarrow O_2(v - 2) + N_2(v = 1) \qquad (10)$$

in which the excited O_2 molecule loses two vibrational quanta ($\Delta E_{v,\,v-2}/hc = 2158$ cm^{-1} and 2208 cm^{-1} for $v = 22$ and 21, respectively) whilst the collision partner gains one ($\Delta E_{v,\,v-1}/hc = 2330$ cm^{-1} for N_2). From the viewpoint of atmospheric chemistry, it is interesting to note that, as the self-relaxation rates of $O_2(v)$ fall to higher v, the rates with N_2 increase so that N_2 acts as the dominant relaxant in the atmosphere for vibrational levels of O_2 above $v \approx 14$.

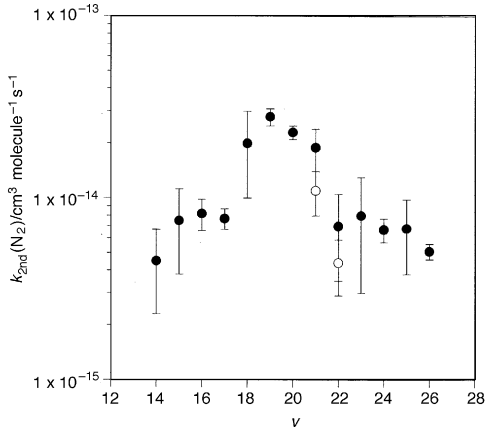

Fig. 9 Comparison of rate constants for the relaxation of $O_2(v)$ by N_2. Results of the present work including estimated uncertainties (○), and the measurements of Mack *et al.*[11] (●).

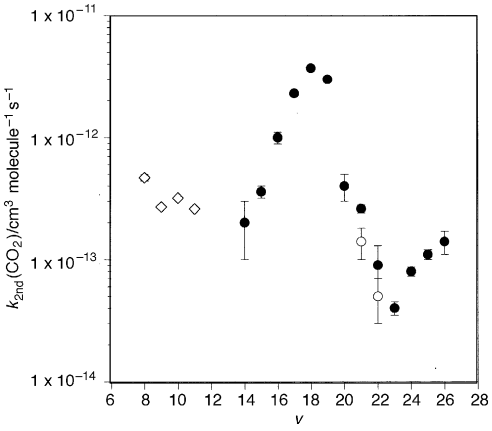

Fig. 10 Comparison of rate constants for the relaxation of $O_2(v)$ by CO_2. Results of the present work including estimated uncertainties (○), the measurements of Mack *et al.*[11] (●) and the results of Klatt and co-workers[12] (▲).

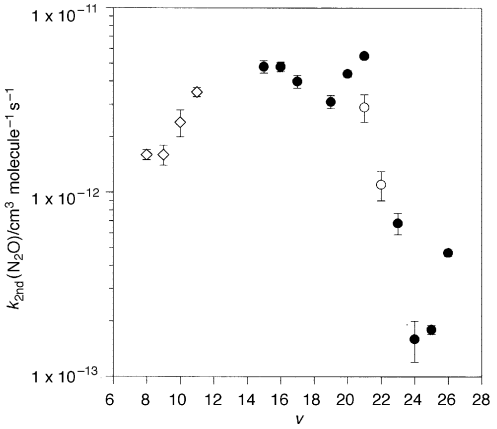

Fig. 11 Comparison of rate constants for the relaxation of $O_2(v)$ by N_2O. Results of the present work including estimated uncertainties (□), the measurements of Mack *et al.*[11] (●) and the results of Klatt and co-workers [12] (▲).

For CO_2, the ν_3 fundamental transition energy is 2349 cm^{-1} which means that the V–V process

$$O_2(v) + CO_2(000) \rightarrow O_2(v - 2) + CO_2(001) \qquad (11)$$

comes into resonance at $v = 18$ where the largest relaxation rate has been found by Mack *et al.*[11] N_2O has an IR-active vibrational mode, ν_1, at 1285 cm^{-1}. Single quantum V–V transfer to this mode from $O_2(v)$ is undoubtedly important at lower v and is responsible for the peak in the plot of rate constants against v at *ca.* $v = 15$. At higher levels, it again appears that processes in which $O_2(v)$ loses two vibrational quanta and N_2O gains one in the ν_3 mode (2224 cm^{-1}) become important.

It is also interesting to compare the maximum values of the rate constants for relaxation by the collision partners N_2, CO_2 and N_2O. Those for $M = CO_2$ and N_2O are roughly two orders of magnitude larger than those for $M = N_2$. These results, like many others, are consistent with the basic ideas of the theory first propounded by Sharma and Brau,[31] according to which V–V energy exchange occurs not under the influence of short-range repulsive forces between the colliding species but rather under the action of the long-range attractive forces and, in particular, by how these forces are modulated by the molecular vibrations. Sharma and Brau[31] developed these ideas into an approximate but quantitative model, in which the long-range intermolecular potential is expressed as a summation of terms incorporating the various electrostatic multipoles on the two collision partners. According to this theory, IR-active vibrations will more readily transfer or accept vibrational quanta than non-active vibrations because they possess a non-zero electric dipole transition moment. The transition moments associated with the ν_3 vibrations in CO_2 and N_2O are particularly strong and explain why they act as much better acceptors of energy from $O_2(v)$ in V–V exchange processes than does N_2. In addition, we note that the rate constants (or collisional probabilities) for all three of these processes are about two orders of magnitude less than might be expected if the molecule giving up energy was undergoing a single quantum transition. This is undoubtedly attributable to the lower transition dipole moment in the case of a transition where two quanta of vibrational energy are transferred.

In the case of CH_4, there are no fundamental transitions in very close resonance with either single or double quantum transitions in $O_2(v)$ for the two vibrational levels studied in the present work. Mack *et al.*[11] do not report rate constants for relaxation by CH_4. Klatt and co-workers[12] attributed the

rapid relaxation of $O_2(v = 8–11)$ (rate constants of *ca.* 10^{-11} cm^3 $molecule^{-1}$ s^{-1}) to V–V transfer to the IR-active fundamental ν_3 mode of CH_4 at 1306 cm^{-1}. By $v = 21$ and 22, this process has become endothermic and less resonant by 215 and 239 cm^{-1}, respectively. The rate constants for relaxation from these levels by CH_4 are substantially less than those of $O_2(v = 8–11)$ which is entirely consistent with our proposal that V–V energy exchange to ν_3 is the dominant mechanism by which CH_4 relaxes $O_2(v)$.

Summary and Conclusions

This paper reports the relative yields of $O_2(X\,^3\Sigma_g^-)$ formed in vibrational levels $18 \leqslant v \leqslant 23$ in the photolysis of O_3 at 266 nm and from the reaction of $O(^1D)$ with O_3. The first of these distributions confirms that vibrationally excited O_2 is generated in all vibrational levels up to the maximum ($v = 22$) which is accessible energetically and that the distribution peaks at $v = 20$. The distribution at these highest levels is not bimodal, in contrast to that found by Miller *et al.*[21] when O_3 is photolysed at 226 nm.

Relaxation rates have been measured for $O_2(X\,^3\Sigma_g^-, v = 21$ and 22) with He, O_2, N_2, CO_2, N_2O and CH_4. Where comparisons with other work are possible the agreement is satisfactory. The absolute values of the rate constants for relaxation are consistent with well established notions in respect of collisional energy transfer. With the molecular collision partners, V–V energy exchange is usually the dominant mechanism even if the resonance is between a two quantum transition in $O_2(v)$ and a single quantum transition in the partner. Moreover, IR-active acceptor modes are clearly more efficient than non-IR-active modes.

From the standpoint of atmospheric chemistry our results confirm that relaxation from high vibrational states of O_2 by the major atmospheric constituents, N_2 and O_2, is much too rapid for the photodissociation of these molecules to contribute significantly to the formation of ozone in the upper atmosphere. The alternative possibility, that the formation of O_2 in vibrational levels $v \geqslant 26$ by photolysis of O_3 could generate $O(^3P)$ atoms, and subsequently O_3, by reaction (9) now also seems to be unlikely, following the finding[32] that the reverse reaction between $O(^3P)$ and O_3 does not yield high concentrations of $O_2(X\,^3\Sigma_g^-, v)$ in vibrational levels close to the energetic limit. Arguments based on the principle of detailed balance then suggest that it is very unlikely that reaction (9) can proceed rapidly. It appears that another mechanism must be found to explain the discrepancy between calculated and observed levels of O_3 in the upper stratosphere and lower mesosphere.

We thank SERC/NERC for support under its Initiative in Laboratory Measurements for Atmospheric Chemistry. K. M. H. is grateful to NERC for the award of a research studentship. We thank Dr R. A. Kennedy for assistance with the calculations of Franck–Condon factors. We thank Professor P. L. Houston and Dr J. Mueller for helpful discussions and for permission to use their results in Fig. 6 prior to publication.

References

1 T. G. Slanger, L. E. Jusinski, G. Black and G. E. Gadd, *Science*, 1988, **241**, 945.
2 (*a*) R. Atkinson, D. L. Baulch, R. A. Cox, R. F. Hampson Jr., J. A. Kerr, M. J. Rossi and J. Troe, *Phys. Chem. Ref. Data*, 1997, **26**, 521; (*b*) W. B. Demore, S. P. Sander, D. M. Golden, R. F. Hampson Jr., M. J. Kurylo, C. J. Howard, A. R. Ravishankara, C. E. Kolb and M. J. Molina, *Chemical and Photochemical Data for Use in Stratospheric Modeling Evaluation Number 11*, NASA JPL-Publication 97-4, 1997.
3 L. Froidevaux, M. Allen and Y. L. Yung, *J. Geophys. Res.*, 1985, **90**, 12999; (b) R. T. Clancy, D. W. Rusch, R. J. Thomas, M. Allen and R. S. Eckman, *J. Geophys. Res.*, 1987, **92**, 3067.
4 NASA Reference Publication 1292, vol. II, *The Atmospheric Effects of Stratospheric Aircraft: Report of the 1992 Models and Measurements Workshops*, March 1993.
5 *Atmospheric Ozone Report*, no. 16, W.M.O., Geneva, 1986.
6 C. A Rogaski, J. A. Mack and A. M. Wodtke, *Faraday Discuss.*, 1995, **100**, 229.
7 R. Toumi, B. J. Kerridge and J. A. Pyle, *Nature* (*London*), 1991, **351**, 217.
8 (*a*) D. Rapp and P. Englander-Golden, *J. Chem. Phys.*, 1964, **40**, 573; (*b*) D. Rapp, *J. Chem. Phys.*, 1965, **43**, 316; (*c*) D. Rapp and T. A. Kassal, *Chem. Rev.*, 1969, **69**, 61.
9 (*a*) H. Park and T. G. Slanger, *J. Chem. Phys.*, 1994, **100**, 287 ; (*b*) T. G. Slanger and R. A. Copeland, in *Advances in Chemical Kinetics and Dynamics*, ed. J. R. Barker, JAI Press, 1994, vol. 2.
10 J. M. Price, J. A. Mack, C. A. Rogaski and A. M. Wodtke, *Chem. Phys.*, 1993, **175**, 83.
11 J. A. Mack, K. Mikulecky and A. M. Wodtke, *J. Chem. Phys.*, 1996, **105**, 4105.
12 (*a*) M. Klatt, I. W. M. Smith, R. P. Tuckett and G. N. Ward, *Chem. Phys. Lett.*, 1994, **224**, 253; (*b*) M. Klatt, I. W. M. Smith, A. C. Symonds, R. P. Tuckett and G. N. Ward, *J. Chem. Soc., Faraday Trans.*, 1996, **92**, 193.
13 G. D. Billing and R. E. Kolesnick, *Chem. Phys. Lett.*, 1992, **200**, 382.
14 R. Hernandez, R. Toumi and D. C. Clary, *J. Chem. Phys.*, 1995, **102**, 9544.
15 I. W. M. Smith, R. P. Tuckett and C. J. Whitham, *Chem. Phys. Lett.*, 1992, **200**, 615.
16 (*a*) W. D. McGrath and R. G. W. Norrish, *Proc. R. Soc.*, 1957, **242**, 265; (*b*) W. D. McGrath and R. G. W. Norrish, *Proc. R. Soc.*, 1960, **254**, 317.
17 (*a*) R. V. Fitzsimmons and E. J. Bair, *J. Chem. Phys.*, 1964, **40**, 451; (*b*) V. D. Baiamonte, L. G. Hartshorn and E. J. Bair, *J. Chem. Phys.*, 1971, **55**, 3617.
18 (*a*) C. B. Cleveland and J. R. Wiesenfeld, *J. Chem. Phys.*, 1988, **89**, 6549; (*b*) M. J. Daniels and J. R. Wiesenfeld, *J. Chem. Phys.*, 1993, **98**, 321.
19 T. Kinugawa, T. Sato, T. Arikawa, Y. Matsumi and M. Kawasaki, *J. Chem. Phys.*, 1990, **93**, 3289.
20 (*a*) C. E. Fairchild, E. J. Stone and G. M. Lawrence, *J. Chem. Phys.*, 1978, **69**, 3632; (*b*) R. K. Sparks, L. R. Carlson, K. Shobatake, M. L. Kowalczyk and Y. T. Lee, *J. Chem. Phys.*, 1980, **72**, 1401.
21 R. L. Miller, A. G. Suits, P. L. Houston, R. Toumi, J. A. Mack and A. M. Wodtke, *Science*, 1994, **264**, 1831.
22 (*a*) P. S. Julienne and M. Krauss, *J. Mol. Spectrosc.*, 1975, **56**, 270; (*b*) P. S. Julienne, *J. Mol. Spectrosc.*, 1976, **63**, 60; (*c*) P. C. Cosby, H. Park, R. A. Copeland and T. G. Slanger, *J. Chem. Phys.*, 1993, **98**, 5117.
23 P. H. Krupenie, *J. Phys. Chem. Ref. Data*, 1972, **1**, 423.
24 R. J. LeRoy, *University of Waterloo Chem. Phys. Res. Rep.* CP-110, 1978.
25 R. S. Friedman, *J. Quant. Spectrosc. Radiat. Transfer*, 1990, **43**, 225.
26 A. S.-C. Cheung, D. K.-W. Mok, Y. Sun and D. E. Freeman, *J. Mol. Spectrosc.*, 1994, **163**, 9.
27 P. L. Houston, personal communication
28 S. T. Amimoto, A. P. Force and J. R. Wiesenfeld, *Chem. Phys. Lett.*, 1978, **60**, 40.
29 (*a*) R. C. Millikan and D. R. White, *J. Chem. Phys.*, 1963, **39**, 3209; (*b*) D. J. Miller and R. C. Millikan, *J. Chem. Phys.*, 1970, **53**, 3384.
30 J. T. Yardley, *Introduction to Molecular Energy Transfer*, Academic Press, New York, 1980.
31 (*a*) R. D. Sharma, *Phys. Rev.*, 1969, **177**, 439; (*b*) C. A. Brau and R. D. Sharma, *J. Chem. Phys.*, 1969, **50**, 924.
32 J. A. Mack, Y. Huang, A. M. Wodtke and G. C. Schatz, *J. Chem. Phys.*, 1996, **105**, 7495.

Paper 7/07569C; *Received* 20*th October*, 1997